 CMES, vol.113, no.3, pp.367-387, 2017

Performance of Compact Radial Basis Functions in the Direct Interpolation Boundary Element Method for Solving Potential Problems

C. F. Loeffle[1], L. Zamprogno[2], W. J. Mansur[3] and A. Bulcão[4]

Abstract: This study evaluates the effectiveness of a new technique that transforms doma in integrals into boundary integrals that is applicable to the boundary element method. Si mulations were conducted in which two-dimensional surfaces were approximated by inter polation using radial basis functions with full and compact supports. Examples involving Poisson's equation are presented using the boundary element method and the proposed te chnique with compact radial basis functions. The advantages and the disadvantages are e xamined through simulations. The effects of internal poles, the boundary mesh refinemen t and the value for the support of the radial basis functions on performance are assessed.

Keywords: Interpolations, radial basis functions, boundary element method, Poisson's equation.

1 Introduction

There are a large number of two-dimensional and three-dimensional engineering problems in which an approximate function must be constructed from known data obtained at certain points. Thus, developments related to techniques such as interpolation and curve fitting have been increasing, particularly for imaging problems, one of the most important applications of this theory.

Regarding the integral techniques focusing to achieve approximate solutions of partial differential equations, many studies have generated different kind of functions as well as several suitable integral models have been examined [Dong, Alotaibi, Mohiuddine and Atluri (2014)].

Radial basis functions (RBFs), which provide a measure of the Euclidian distance between base points and domain points, are a very important tool in this context. More detailed discussions of RBFs and the modern theory of approximation can be found in the literature [Buhmann(2003); Fasshauer (2007); Sarra and Kansa (2009)]. Initially, RBFs were used mostly for the interpolation of scattered data, particularly with certain discrete methods. For example, the dual reciprocity boundary element method (DRBEM) uses

[1] DEM/PPGEM, Federal University of Espírito Santo, carlos.loeffler@ufes.br (corresponding author).

[2] PGSU Petrobras, lorenzo.souza@petrobras.com.br.

[3] PEC/LAMEMO/COPPE/Federal University of Rio de Janeiro, webe@coc.ufrj.br.

[4] CENPES Petrobras, bulcao@petrobras.com.br.

RBFs for interpolation of the domain actions (Loeffler and Mansur, 1986). More recently, RBFs have been used in mesh-free formulations of the finite element method (FEM). In this approach, the elements or cells are not required to delimit or connect the degrees of freedom defined by the discretisation [Atluri and Zhu (2000); Wang and Liu (2002)].

Thus, one of the most effective ways to generate both the points of discretisation and to correlate the areas of influence is through the use of a special class of radial functions for local approximations, the compactly supported radial basis function (CSRBF) [Wendland (1995); Wu (1995); Floater and Iske (1996)]. Because the range of each function associated with a base point is restricted, this type of function is desirable for reducing the computations required to solve systems of equations in the FEM by transforming a fully sparse matrix into a banded matrix. This method also reduces the risk of poor conditioning of the problem by creating diagonally dominant interpolation matrices.

Concerning applications of the DRBEM, CSRBFs also present advantages over the traditionally used complete radial basis functions, especially in ill-conditioned problems in which the interpolation matrix involves a large number of basis points [Chen, Brebbia and Power (1999)]. In fact, computational tests have shown that many classical complete radial basis functions are inadequate for the DRBEM in certain applications. Several studies found a lack of convergence when traditional complete radial functions were used in the DRBEM in conjunction with iterative procedures [Cheng, Young and Tsai (2000)]. It should be emphasised that the use of radial functions in the DRBEM differs from the simple interpolation procedure and the techniques of solving differential equations because it generates two primitive functions from the original interpolation function [Partridge, Brebbia and Wrobel (1992)], forming auxiliary matrices that may produce additional undesirable numerical effects.

It must be highlighting that comparisons between numerical techniques to solve suitably domain integrals have been continually performed, examining many different and important engineering branches. Ekhlakov et al. (2013) evaluate the domain integral that appears in transient thermoelastic crack analysis in functionally graded materials using three techniques: the standard cell integrations, the Cartesian transformation method as well as the radial integration method.

In this study, a new BEM technique, the direct interpolation boundary element method (DIBEM), is developed to solve domain integrals. This method is original and differs from the DRBEM in that it is simpler and closely resembles an interpolation procedure despite the use of primitive radial functions in the transformation of the domain integrals into boundary integrals. The DIBEM was successfully applied to problems involving the solution of Poisson's equation using classical RBFs [Loeffler, Cruz and Bulcão (2015)].

Initially, CRBFs are used to solve examples related to the calculation of the volume below the surfaces generated numerically by interpolation to assess their performance. Based on these results, it became possible to identify the best CRBFs for solving two problems involving Poisson's equation. Solving these problems provides insight regarding the value of support and the loss of accuracy.

2 Poisson's boundary integral equation

A solution to Poisson's equation is sought, where it is assumed that the problem is two-dimensional, physically homogeneous and isotropic. A body action p(X) exists inside the domain Ω(X), which is limited by a boundary Γ(X), where are imposed prescribed potential conditions on Γ_u(X) and potential normal derivatives q(X) on complementary boundary Γ_q(X).

Given an auxiliary function u*(ξ; X) and its normal derivative q*(ξ; X), where ξ is an arbitrary point, an equivalent integral form of Poisson's equation, given by Brebbia, Telles and Wrobel (1984), can be written

$$c(\xi)u(\xi)+\int_{\Gamma}u(X)q^{*}(\xi;X)d\Gamma-\int_{\Gamma}q(X)u^{*}(\xi;X)d\Gamma=-\int_{\Omega}p(X)u^{*}(\xi;X)d\Omega \qquad (1)$$

The auxiliary function u*(ξ;X) is referred to as the fundamental solution. In Eq. 1, the value of the coefficient c(ξ) depends on both the position of the point ξ with respect to the physical domain Ω(X) and the boundary smoothness at this point [Wrobel and Aliabadi (2002)]. The standard BEM procedure requires the implementation of a process in which the source points must be located on the boundary. The domain integral on the right-hand side of Eq. 1 is the focus of the boundary transformation given by the DIBEM.

3 DIBEM procedure for poisson's equation

The goal is to solve the aforementioned domain integral term without resorting to standard techniques such as cells. Thus, an interpolation using radial basis functions is performed in an approach that is similar to the DRBEM procedure. However, the complete kernel of the domain integral is interpolated directly according to the following expression:

$$p(X)u^{*}(\xi;X)=z(\xi;X)=F^{j}(X^{j};X)^{\xi}\alpha^{j} \qquad (2)$$

The function $F^j(X^j; X)$ is composed of radial basis functions. For each source point ξ, the interpolation given by Eq. 2 is performed for all of the base points X^j in relation to the domain or information points X and weighted by the coefficients ${}^{\xi}\alpha^j$. The number of basis points X^j must be equal to the number of known values of z (ξ; X). Thus, the ${}^{\xi}\alpha^j$ coefficients can be obtained through the solution of a system of algebraic equations.

In the DIBEM procedure, Eq. 2 is substituted into the domain integral given in Eq. 1 using an auxiliary primitive function $\Psi^j(X^j; X)$:

$$\int_{\Omega}z(\xi;X)d\Omega=\int_{\Omega}({}^{\xi}\alpha^{j}\psi^{j}_{,ii}(X^{j};X))d\Omega=\int_{\Gamma}({}^{\xi}\alpha^{j}\psi^{j}_{,i}(X^{j};X)n_{i}(X))d\Gamma= {}^{\xi}\alpha^{j}\int_{\Gamma}\eta^{j}(X^{j};X)d\Gamma \qquad (3)$$

The DIBEM approach is very similar to an interpolation procedure and makes use of only a primitive function. Because the mathematical demands of the proposed method are less

stringent than those of the DRBEM, the proposed method tends to have better performance. For well-known classical RBFs, the DIBEM is always convergent with the mesh refinement, whereas the DRBEM is not. Its occurs due the DIBEM approximates directly the complete kernel, similarly to what is done in the interpolation procedure, making use of only a primitive function. Just the transformation of the domain integral into a boundary integral makes the DIBEM different to a basic interpolation procedure. It may happen that certain well-known classical RBFs may yield better performance than other functions if they are sufficiently similar to the kernel to be approximated.

The numerical evaluation of the boundary integral is very simple. Using Eq. 3 and the well-known BEM procedure for the discretisation, Eq. 1 may be rewritten as follows:

$$\begin{aligned}
&H_{11}u_1 + ...H_{1n}u_n - \ G_{11}q_1 - ....G_{1n}q_n = {}^1\alpha^1 N_1 + {}^1\alpha^2 N_2 + ..{}^1\alpha^n N_n \\
&H_{21}u_1 + ...H_{2n}u_n - \ G_{21}q_1 - ....G_{2n}q_n = {}^2\alpha^1 N_1 + {}^2\alpha^2 N_2 + ..{}^2\alpha^n N_n \\
&..... \\
&H_{n1}u_1 + ...H_{nn}u_n - \ G_{n1}q_1 - ....G_{nn}q_n = {}^n\alpha^1 N_1 + {}^n\alpha^2 N_2 + ..{}^n\alpha^n N_n
\end{aligned} \tag{4}$$

which can be written, in matrix form for convenience, as indicated below:

$$\mathbf{[H]\{u\} - [G]\{q\} = [A]\{N\} = \{P\}} \tag{5}$$

In Eq. 5, the vectors ${}^{\xi}\boldsymbol{\alpha}$ that form the columns of matrix **A** may be obtained from the basic interpolation equation:

$$\mathbf{[F][}{}^{\xi}\boldsymbol{\alpha}\mathbf{] = [}{}^{\xi}\boldsymbol{\Lambda}\mathbf{]u} \tag{6}$$

In Eq. 6, the values of the fundamental solution comprise the matrix ${}^{\xi}\boldsymbol{\Lambda}$**.** For each source point ξ, the right-hand side of Eq. (6) may be rewritten as follows:

$$\mathbf{[}{}^{\xi}\boldsymbol{\Lambda}\mathbf{][u] = [}{}^{\xi}\boldsymbol{\Lambda}\mathbf{][F]}\boldsymbol{\alpha} \tag{7}$$

Solving Eq. 6 for ${}^{\xi}\boldsymbol{\alpha}$ and substituting the result displayed in Eq. (7) gives

$$\mathbf{[}{}^{\xi}\boldsymbol{\alpha}\mathbf{] = [F]^{-1}[}{}^{\xi}\boldsymbol{\Lambda}\mathbf{][F]}\boldsymbol{\alpha} = \mathbf{[F]^{-1}[}{}^{\xi}\boldsymbol{\Lambda}\mathbf{][p]} \tag{8}$$

For problems involving Poisson's equation, it is possible to reduce the computations because the matrix ${}^{\xi}\boldsymbol{\Lambda}$ is diagonal. In both boundary element methods, i.e., the DRBEM and the DIBEM, the inverse of a matrix must be computed once. However, the DRBEM requires construction of the two interpolation matrices and products that involves matrices **H** and **G**, which are full matrices [Partridge, Brebbia and Wrobel (1992)]. The DIBEM reduces the computational time because only the product of ${}^{\xi}\boldsymbol{\Lambda}$ and $\mathbf{F}^{-1}$ is required for each source point.

The impossibility of choosing the points X in coincidence with the source points to avoid singularities is another important feature of the DIBEM, because the fundamental

solution forms the kernel. In consequence, using linear boundary elements, the body force values p (X) is taken at the centre. Concerning to the interpolation, the points X^i can coincide with the nodal points X in the approximation of the domain integral, for sake of simplicity.

4 Radial basis functions with global support

Modern approaches commonly approximate the source variable z(X) as a sum of two functions as follows:

$$z(X) \approx F^j(X^j;X)\alpha^j + B^i(X)\beta^i \quad i=1,\ldots,K; \quad j=1,\ldots..L \tag{9}$$

In Eq. 9, the radial basis functions F^j are added to the polynomial functions B^i, which are composed of the following monomial terms:

$$\mathrm{B^i(X)} = [1, \mathrm{x}, \mathrm{y}, \mathrm{x^{2,}}, \mathrm{xy}, \mathrm{y^2}, ...] \tag{10}$$

Unlike the radial basis functions, the monomial terms have the origin of the coordinate system as a reference. (There is an additional requirement that the approximation is unique, that is) An additional requirement for uniqueness of the approximation is:

$$B^i(X)\beta^i = 0 \tag{11}$$

This set of polynomial functions was introduced and adapted to the DRBEM formulation by Golberg and Chen (1994). These functions are effective in many applications, especially if the source term behaves in accordance with the monomial. However, for body forces with more complex shapes, polynomial functions should be used together with radial basis functions. Concerning the DIBEM, the interpolated kernel is not a polynomial function as a rule because it is given by the product of the source term p(X) by the fundamental solution. Indeed, in two-dimensional problems, the Laplace's fundamental solution is given by a logarithm; thus, it is possible to infer that a logarithmic radial basis function gives good results for this class of problems. However, this study discards polynomials functions, despite the possibility that their use might improve the performance and focuses on non-classical radial basis functions, used specially with the modern meshless techniques: the compact radial basis functions (CRBFs).

5 Compact radial basis functions

CBRFs are a specific class of RBFs which are nonzero only for values of the Euclidian distance r less than a previously selected value of the support parameter δ. In general, CRBFs are expressed by:

$$\mathrm{F^j}\left(\frac{\mathrm{r}}{\delta}\right) = \phi_{\mathrm{l,k}}\,\mathrm{p}\left(\frac{\mathrm{r}}{\delta}\right) \tag{12}$$

The truncated power function $\Phi_{l,\,u}$ in Eq. 12 satisfies the following conditions:

$$\phi_{l,k} = \left(1 - \frac{r}{\delta}\right)_+^l = \begin{cases} \left(1 - \frac{r}{\delta}\right)^l, & 0 \le r \le \delta \\ 0, & r > \delta \end{cases} \tag{13}$$

It can easily be verified that the CRBF is truncated at zero for r greater than the compact support value δ. The indexes l and k represent the spatial dimension and the function smoothness, respectively, and the polynomial term $p(\frac{r}{\delta})$ is prescribed by mathematical recurrence relations that characterise the various classes of CRBFs.

Twelve CRBFs were examined: eight Wendland functions [Wendland (1995)] and four Wu functions [Wu (1995)], which are given in Table 1. Complete lists of these functions may be found in the literature [Schaback (2007)].

Table 1: CRBFs used in the interpolation tests

Wendland CRBF's:	Wu CRBF's:
$\Phi_{1,0}(r) \doteq \left[1-\frac{r}{\delta}\right]_+$	$\Phi_{3,3}(r) \doteq \left[1-\frac{r}{\delta}\right]_+^4\left[16+29\frac{r}{\delta}+20\left(\frac{r}{\delta}\right)^2+5\left(\frac{r}{\delta}\right)^3\right]$
$\Phi_{3,0}(r) \doteq \left(1-\frac{r}{\delta}\right)_+^2$	$\Phi_{2,3}(r) \doteq \left[1-\frac{r}{\delta}\right]_+^5\left[8+40\left(\frac{r}{\delta}\right)+48\left(\frac{r}{\delta}\right)^2+25\left(\frac{r}{\delta}\right)^3+5\left(\frac{r}{\delta}\right)^4\right]$
$\Phi_{5,0}(r) \doteq \left[1-\frac{r}{\delta}\right]_+^3$	
$\Phi_{1,1}(r) \doteq \left[1-\frac{r}{\delta}\right]_+^3\left[1+3\frac{r}{\delta}\right]$	$\Phi_{1,3}(r) \doteq \left[1-\frac{r}{\delta}\right]_+^6\left[6+36\frac{r}{\delta}+82\left(\frac{r}{\delta}\right)^2+72\left(\frac{r}{\delta}\right)^3+30\left(\frac{r}{\delta}\right)^4+5\left(\frac{r}{\delta}\right)^5\right]$
$\Phi_{3,1}(r) \doteq \left[1-\frac{r}{\delta}\right]_+^4\left[1+4\frac{r}{\delta}\right]$	
$\Phi_{1,2}(r) \doteq \left[1-\frac{r}{\delta}\right]_+^5\left[1+5\frac{r}{\delta}+8\left(\frac{r}{\delta}\right)^2\right]$	
$\Phi_{3,2}(r) \doteq \left[1-\frac{r}{\delta}\right]_+^6\left[35\left(\frac{r}{\delta}\right)^2+18\frac{r}{\delta}+3\right]$	$\Phi_{0,3}(r) \doteq \left[1-\frac{r}{\delta}\right]_+^7\left[5+35\frac{r}{\delta}+101\left(\frac{r}{\delta}\right)^2+147\left(\frac{r}{\delta}\right)^3+101\left(\frac{r}{\delta}\right)^4+35\left(\frac{r}{\delta}\right)^5+5\left(\frac{r}{\delta}\right)^6\right]$
$\Phi_{3,3}(r) \doteq \left[1-\frac{r}{\delta}\right]_+^8\left[32\left(\frac{r}{\delta}\right)^3+25\left(\frac{r}{\delta}\right)^2+8\frac{r}{\delta}+1\right]$	

The use of CRBFs with the DIBEM implies on the boundary integration path being delimited by the support circumference. In general, the source point may be located on the boundary or internally so that the extension of the support radius involves physical boundaries, and the integration path is composed of separate parts, as shown for example in Figure 1:

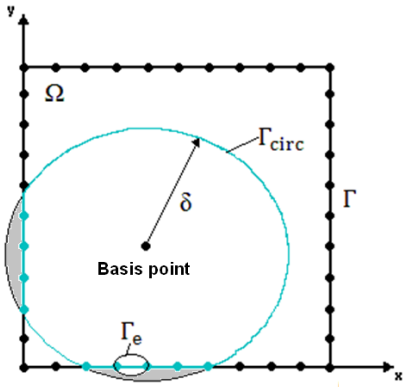

Figure 1: Boundary integration path delimited by the support radius, which is centred internally

6 Internal basis points

An accurate distribution of the body action p(X) inside the domain requires the insertion of internal interpolation basis points. Because the DIBEM directly interpolates all functions that comprise the kernel of the integral, a larger number of these internal points are necessary for better performance. The importance of internal basis points remains if CRBFs are used because a sufficient number of internal points must be located internally for each circle delimited by the support.

7 Validation tests

The objective of the validation tests is to evaluate the effectiveness of the proposed procedure for solving the boundary integral for a basic interpolation problem before simulating the BEM models. These tests offer an excellent opportunity to evaluate the performance of the DIBEM procedure, to discuss certain features of the radial functions introduced by Wu and Wend land and choose the most suitable functions. Choosing the proper class of functions and the support radius requires a degree of skill and experience, so the examples provide an important guideline.

The volume under the two-dimensional surface is calculated using the boundary integral. Surfaces are approximated by a linear set of compact radial basis functions, and their interpolation points are uniformly distributed on a mesh. At these points known data are collected. Intermediate values are established by interpolation. Tests were conducted with two distinct functions, Franke's function [Franke (1982)] and a paraboloid, which are given by Eq. 14 and Eq. 15, respectively:

$$z(x,y) = 0{,}75e^{-0{,}25(9x-2)^2-0{,}25(9y-2)^2} + 0{,}75e^{-(9x-2)^2/49-(9y-2)^2/10} + 0{,}7e^{-0{,}25(9x-7)^2-0{,}25(9y-3)^2} - 0{,}2e^{-(9x-4)^2-(9y-7)^2} \quad (14)$$

$$z(x,y) = [(x-0{,}5)^2 + (y-0{,}5)^2]^{1/2} \quad (15)$$

The proposed domain is a square with unity side length dimensions. Figure 2 shows a typical example of a mesh. Forty points were chosen on the boundary. The relative positions of the base points (located internally) are shown.

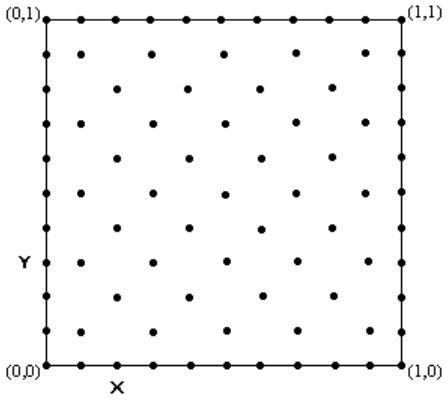

Figure 2: Example mesh with forty boundary basis points and thirty-nine internal basis points

Other meshes with similar proportions between the numbers of base points on the boundary and inside the domain were used for the simulations, as given in Table 2. Finer meshes were tested to examine the convergence of the proposed procedure.

Table 2: Numbers of boundary and internal basis points for each mesh tested

Boundary	8	16	24	32	40	48	56	64	72	80	88	96	104	112	120	128	136	144	152	160
Internal	1	5	13	25	41	61	85	113	145	181	221	265	313	365	421	481	545	613	685	761
Total	9	21	37	57	81	109	141	177	217	261	309	361	417	377	541	609	681	757	837	921

Referring to Eq. 2, z (x, y) defines a two-dimensional surface that must be approximated in a domain Ω(X). According to the integral transformation given by Eq. 3, the volume V is calculated by evaluating the boundary integral, that is

$$V = \int_{\Omega} z(x,y)d\Omega(x,y) \cong \int_{\Omega} [F^j(x,y)\alpha^j]d\Omega(x,y) = \int_{\Gamma} (\alpha^j \eta^j(X))d\Gamma \quad (16)$$

The boundary integral was evaluated using the Gauss quadrature, which is commonly used with the BEM. Values of the primitive functions $\psi^j(X)$ can be obtained by solving the following ordinary differential equation given in polar coordinates:

$$\frac{d^2\psi}{dr^2} + \frac{1}{r}\frac{d\psi}{dr} = F^j(r) \quad (17)$$

Thus, the following tests will determine whether the primitive functions related to CRBFs have good properties for approximations. In fact, not all functions perform well, as was the case in tests conducted with many classical RBFs. As shown herein later on, certain functions introduced by Wu and Wendland presented numerical problems. In particular, high-order functions tend to produce numerical instabilities. Absence of monotonicity was also observed with certain functions, but no clear reason was found.

7.1 Tests using RBFs with complete support

The twelve CRBFs presented in Table 1 were used to interpolate the surface functions given in Eq. 14 and Eq. 15 using complete support. After identifying the best functions, tests with various degrees of support were conducted. The relative error was determined using the analytical solution as the reference.

7.1.1 Tests with franke's function

Evaluating the boundary integral in Eq. (3), approximate values of the volume for Franke's function were obtained. The relative errors for the two best Wendland and Wu CRBFs are given in Figure 3.

The results were reasonable for these functions because the percentage errors are less than 2% for meshes with more than 150 basis points. In fact, there was no expectation that the accuracy of the boundary integral scheme would be superior to standard domain integration techniques. However, in more advanced applications of the DIBEM, other advantages may compensate the loss of accuracy in addition of the restriction of the discretisation to the boundary.

It must be emphasised that the performance of the functions with higher orders was not satisfactory. For the worst functions, the relative error curves were not monotonic or convergent, as shown in Figure 4 for the Wendland and Wu radial functions with the highest order.

Because complete support was used, examples using meshes without internal poles were tested. If basis points were selected exclusively on the boundary, it would not be possible to adequately represent the surface within the domain, even with the best radial functions because the curves of percentage error converged to incorrect stationary values.

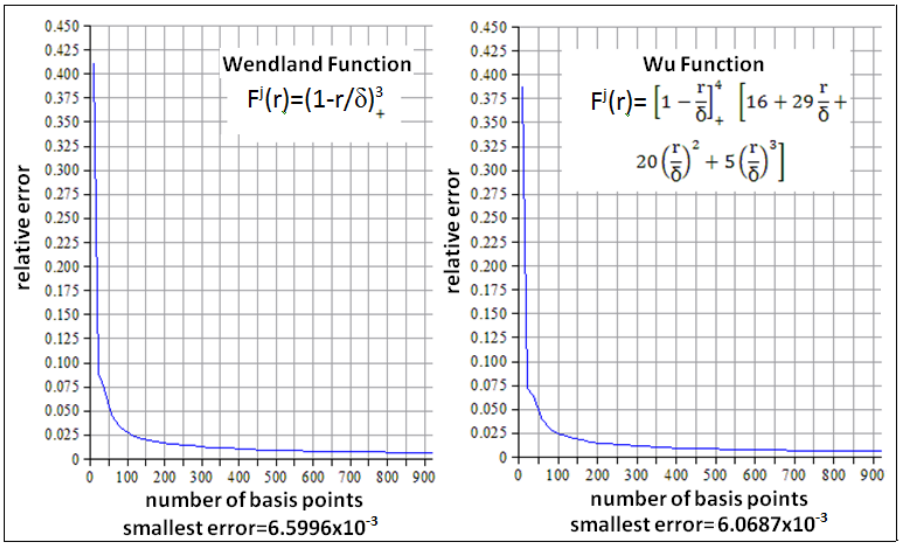

Figure 3: Relative error vs. the number of basis points with the two best functions for interpolation of Franke's function in the volume calculation

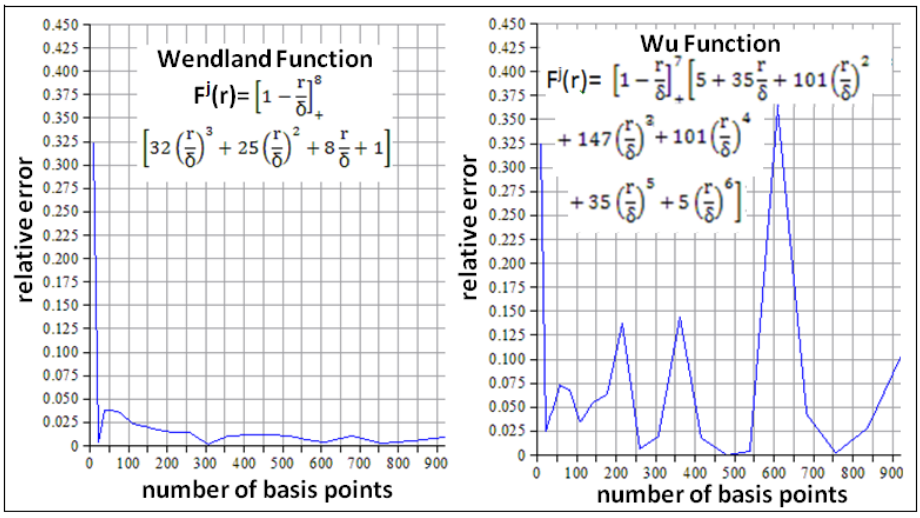

Figure 4: Relative error vs. the number of basis points with the two worst functions in the interpolation of Franke's function for the volume calculation

7.1.2 Tests with the paraboloid

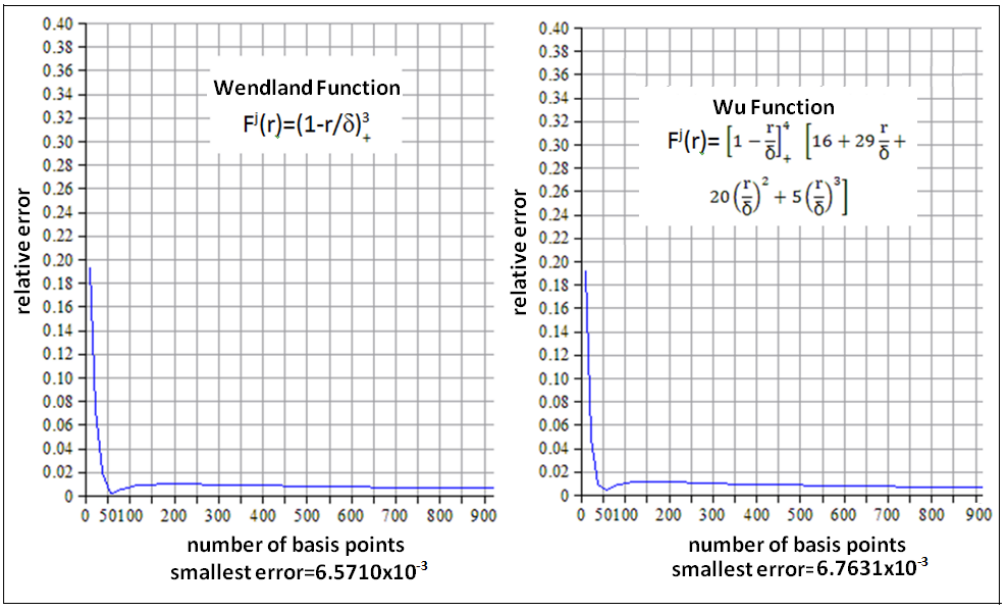

Figure 5: Relative error vs. the number of basis points with the two best functions in the interpolation of the paraboloid for the volume calculation

The best CRBFs were the same as in the previous test. The low levels of relative error demonstrate the accuracy of these classes of functions in approximating the volume using the proposed scheme, particularly if simpler surfaces are involved. The slightly non-monotonic behaviour of the error curves seems to indicate that a minimum value was reached with a few basis points, as shown in Figure 5.

The magnitude of the final error was less for other functions, except those of higher order. However, these functions were not stable as the mesh refinement, or they produced coarse results, especially the Wu functions, as shown previously with the Franke's function results.

7.2 CRBFs with varying levels of support

The following tests evaluate the performance of the proposed procedure with various degrees of support. It is expected that there is a minimum value of the support that results in satisfactory accuracy and reasonable computational costs. Naturally, this minimum value must be greater than that usually found in meshless FEM approaches because of the approximations introduced by the divergence theorem being applied in association with a primitive interpolation function.

The best CRBFs were chosen considering the previous tests results. To evaluate the performance of each CRBF, a fine mesh with 961 basis points regularly distributed in the domain field was used in addition to a coarse mesh with 121 basis points. The support was decreased successively from the complete value to the minimum, at which point satisfactory accuracy was lost.

7.2.1 Tests with Franke's function

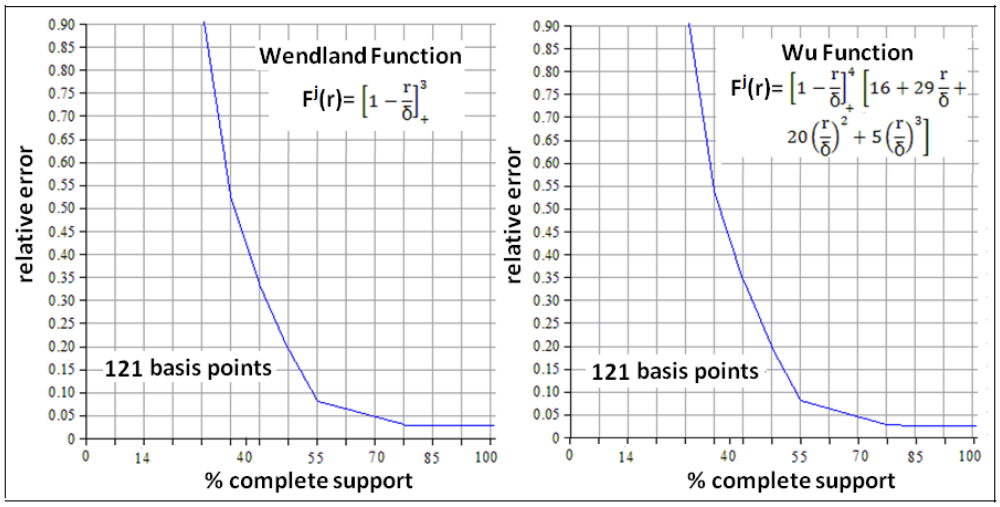

Figure 6: Relative error vs. the percentage of complete support with the two best CRBFs for volume calculations in the interpolation of Franke's function-coarse mesh

The performance of the two best CRBFs was similar for the coarse mesh, as shown in Figure 6. However, the mesh refinement for this case seems to be more effective for the Wu function, particularly to better establish a suitable minimal support; i.e., from this minimum value, the error increases significantly. For the fine mesh, this value is approximately 70% of the global support for both CRBFs, as shown in Figure 7.

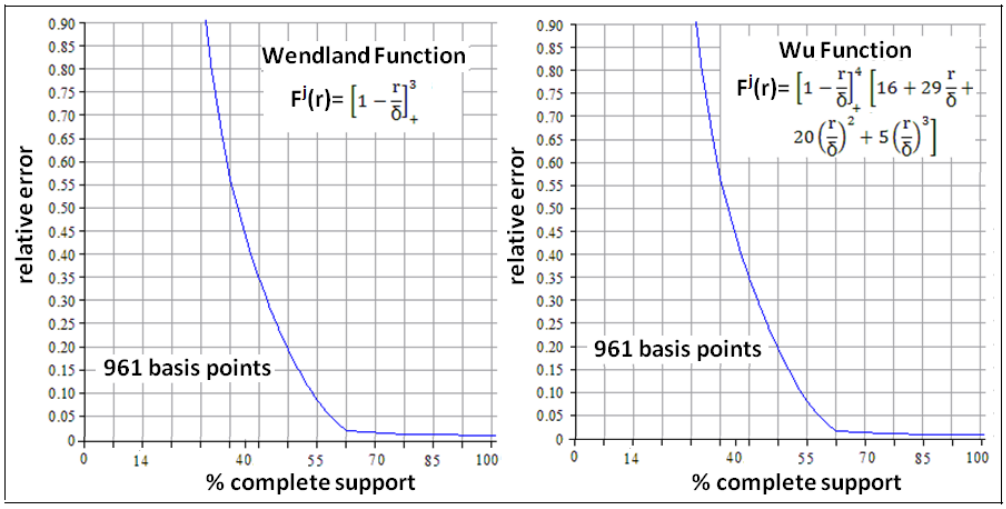

Figure 7: Relative error vs. the percentage of complete support with the two best CRBFs for volume calculations in the interpolation of Franke's function-fine mesh

7.2.2 Tests with the paraboloid

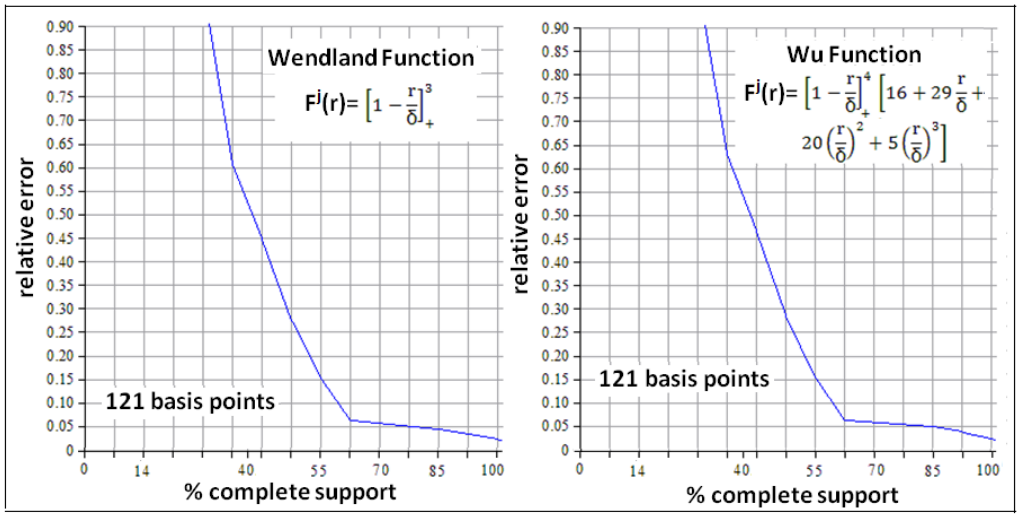

Figure 8: Relative error vs. the percentage of complete support with the two best CRBFs for volume calculations in the interpolation of the paraboloid function-simple mesh

Figure 8 presents the results for the paraboloid using the simple mesh. It can be observed that the accuracy decreases quickly with the reduction of the support. For the fine mesh, the results improve significantly, and the limit where the error curve sharply increases appears clearly at approximately 65% of the complete support value, as shown in Figure 9. Once more, the behaviour of the best CRBFs tested was similar; however, the Wu function appears less efficient for coarse meshes.

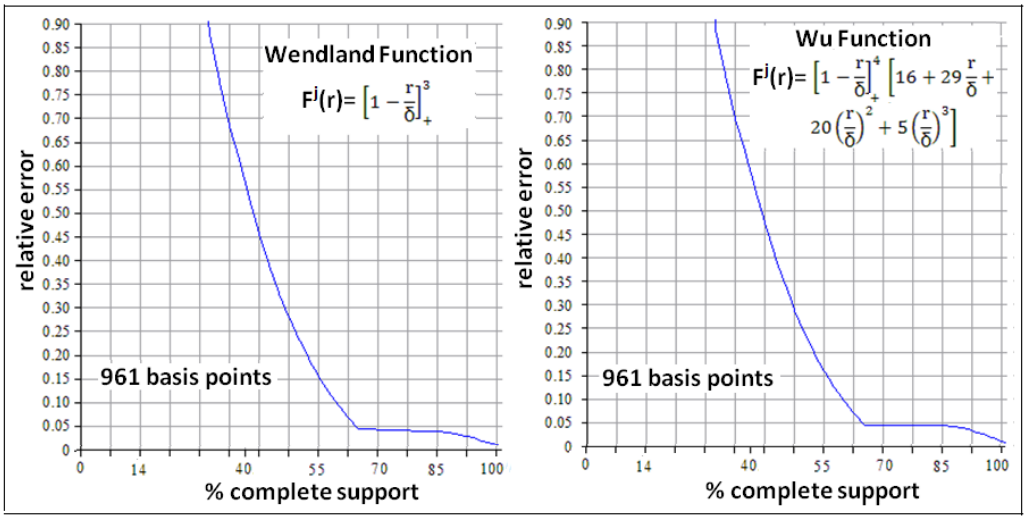

Figure 9: Relative error vs. the percentage of complete support with the two best CRBFs for volume calculations in the interpolation of the paraboloid function-fine mesh

Compared with the results of the previous test with Franke's function, the accuracy was inferior. Other studies have shown that radial basis functions have more difficulty approximating certain simple functions than other, more complex functions such as Franke's function.

8 BEM integration tests

In this section, the solutions of three examples of Poisson's equation in which the DIBEM models the source term are presented. The average percent error was obtained using analytical results as the reference.

Only the results obtained with the best Wend land and Wu CRBFs from the previous section are shown. As occurred in the previous simulations, many functions were not efficient. Some produced poor results, resulting in either numerical instability or intense oscillations.

8.1 Bar subjected to a sinusoidal axial force

In the first example, a sinusoidally distributed axial load is assumed to act on a vertically suspended bar, as shown in Figure 10.

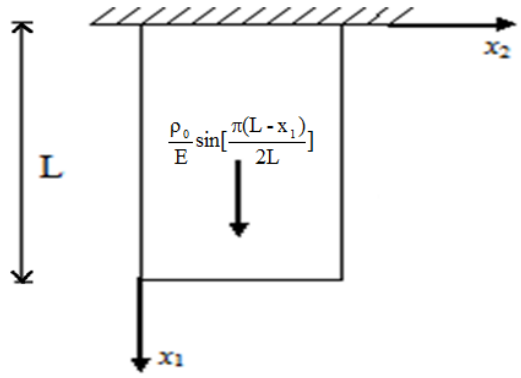

Figure 10: Homogeneous vertical bar subjected to a sinusoidal axial force

The governing equation for this one-dimensional case is given by:

$$\frac{d^2u}{dx_1^2} = \frac{\rho_0}{E}\sin[\frac{\pi(L - x_1)}{2L}] \tag{18}$$

A regular mesh with 164 boundary nodes and 81 internal points was used. The curves presented in Figure 11 show the behaviour of the percent error in the solution of the displacement for some percentage values of the complete support. Function 1 is a Wendland function, and function 2 is a Wu function.

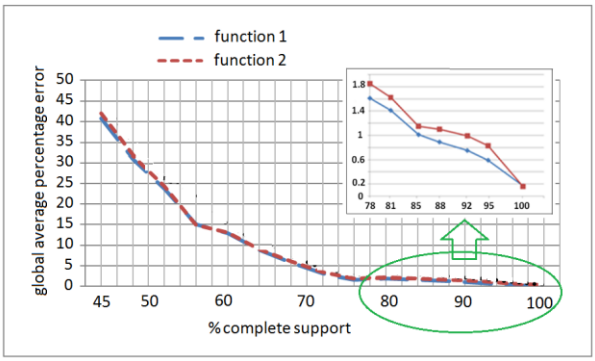

Figure 11: The DIBEM error in displacement vs. the percentage of complete support for two CRBFs using a mesh with 164 boundary nodes and 81 internal poles

It may be pointed out the monotonic behaviour of all two functions during the interval chosen for simulations, varying since the global support until 45% of this value. The results for complete support were very good, with an error of approximately 0.2%. Although there was a noticeable loss of accuracy relatively to the previous tests to volume calculation problems, the results may be considered reasonable, since the percentage values of support are greater than 75%. Because a boundary transformation is performed as part of the DIBEM, the range of acceptable values and the accuracy is strongly reduced compared with the values usually obtained with meshless FEM techniques.

Better results for smaller percentage values of the complete support can be achieved if finer meshes are used. Thus, two new meshes were tested for this demonstration, the first containing a larger number of internal basis points and the second containing more boundary base points. Only the Wendland function was applied in both situations. The results in Figure 12 show that the errors decreased significantly, and the introduction of base points on the boundary was more effective in this case in which the domain force is a smooth function. Indeed, the use of a greater number of boundary nodes has a double effect: improves the numerical approximation of the BEM model as well as the interpolation performed by the radial basis functions.

Results in Figure 12 also can be compared with data presented in detail in Figure 11. It can be inferred that the loss of accuracy incurred using a reduced value of support with a fine mesh is less than that obtained with the coarse mesh using full value of support. Moreover, the computational cost could be significantly lower in this case.

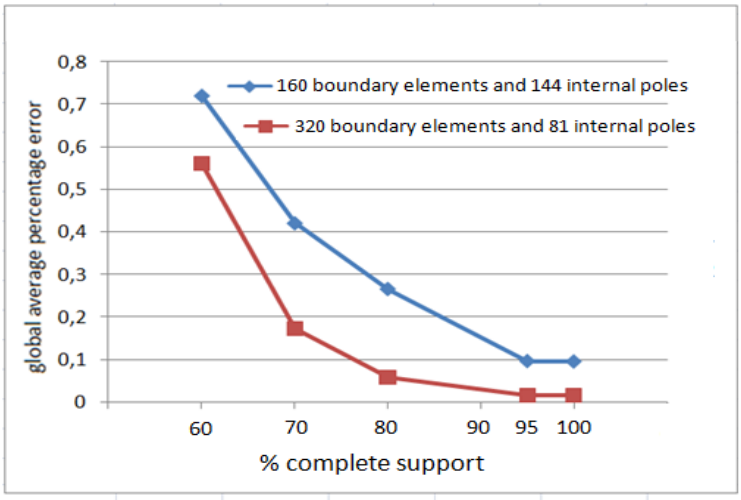

Figure 12: Error in displacements vs. the percentage of complete support for two fine meshes with the Wendland function

8.2 Membrane with one deflected edge subjected to a variable force

This example consists of a two-dimensional problem in which a square membrane with sides of unit length is submitted to a variable distributed force; the governing equation is given by:

$$\nabla^2 u(x_1, x_2) = 6x_1x_2(1-x_2) - 2x_1^3 \tag{19}$$

Three sides are clamped, and the fourth side has the following prescribed normal derivative (i.e., slope):

$$q(1, x_2) = 3x_2(1-x_2) \tag{20}$$

Figure 13 shows the membrane with the imposed boundary conditions.

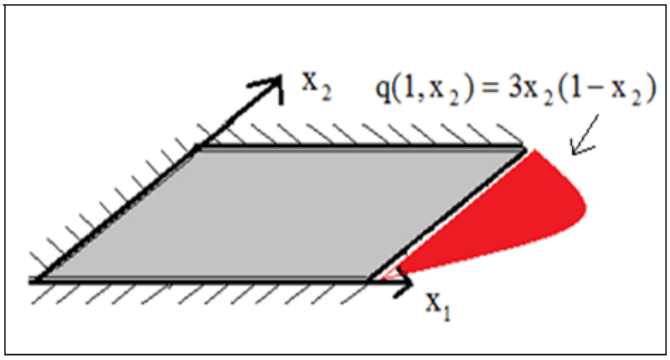

Figure 13: Membrane with Neumann condition prescribed in one side

The analytical solution for the displacement u (x_1, x_2) is given by

$$u(x_1, x_2) = x_2(1-x_2)x_1^3 \tag{21}$$

Despite the relatively smooth variation of the domain force, it is strongly concentrated on the corners, which creates additional difficulties in an interpolation with radial functions. Again, the best Wu and Wendland CRBFs performed similarly, so only the Wendland results are shown for the three meshes. The behaviour of the relative error with the percentage of complete support is very different from that in the previous problem, as can be observed in Figure 14.

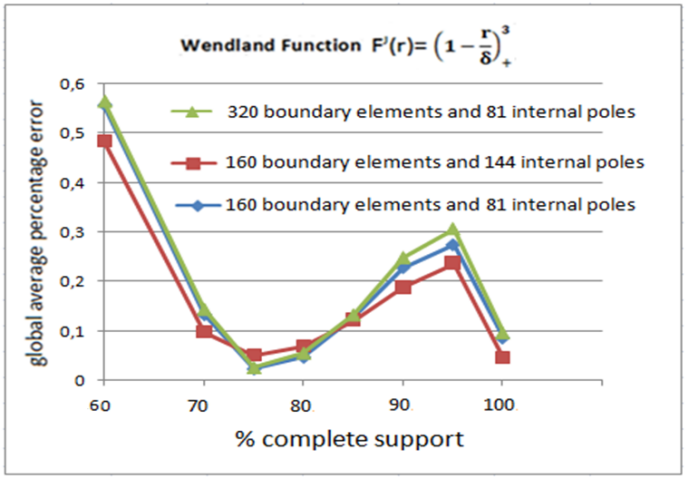

Figure 14: Error in displacements vs. the percentage of complete support for three different meshes

Three different meshes were used for testing, but for all of the meshes the same curious behaviour was observed: as the percentage value of support was reduced, the accuracy initially decreased and then increased such that the error was comparable to that obtained with full support. As the percentage value of the complete support was reduced further, below 75%, the error increased monotonically again.

Unlike the previous example, the inclusion of a greater number of internal points was more effective, then the insertion of poles on the boundary. Certainly, this behaviour occurs because the problem is two-dimensional and has a more complex distribution of the source term, which allows an optimum approximation for the domain action to be obtained with a reduced value for the support.

8.3 Membrane subjected to a complex distributed domain force

The previous example showed that the use of CRBFs with the DIBEM in two dimensions required greater effort to produce better accuracy. Further examination of the effect of support reduction in the interpolation procedure is warranted. In this example, a complex forcing function is applied on the domain of the square membrane. The governing equation is given by:

$$\nabla^2 u(x_1,x_2) = -\frac{751\pi^2}{144}\sin(\frac{\pi x_1}{6})\sin(\frac{7\pi x_1}{4})\sin(\frac{3\pi x_2}{4})\sin(\frac{5\pi x_2}{4}) +$$
$$+\frac{7\pi^2}{12}\cos(\frac{\pi x_1}{6})\cos(\frac{7\pi x_1}{4})\sin(\frac{3\pi x_2}{4})\sin(\frac{5\pi x_2}{4}) +$$
$$+\frac{15\pi^2}{8}\sin(\frac{\pi x_1}{6})\sin(\frac{7\pi x_1}{4})\cos(\frac{3\pi x_2}{4})\cos(\frac{5\pi x_2}{4}) + \quad (22)$$

The boundary conditions are given by the following expressions:

$$u(x_1,1) = -\frac{1}{12}\sin(\frac{\pi x_1}{6})\sin(\frac{7\pi x_1}{4})$$
$$u(1,x_2) = -\frac{1}{2\sqrt{2}}\sin(\frac{3\pi x_2}{4})\sin(\frac{5\pi x_2}{4})$$
$$u(x_1,2) = -\sin(\frac{\pi x_1}{6})\sin(\frac{7\pi x_1}{4})$$
$$u(2,x_2) = -\frac{\sqrt{3}}{2}\sin(\frac{3\pi x_2}{4})\sin(\frac{5\pi x_2}{4}) \quad (23)$$

The exact solution of this problem is given by

$$u(x_1,x_2) = \sin(\frac{\pi x_1}{6})\sin(\frac{7\pi x_1}{4})\sin(\frac{3\pi x_2}{4})\sin(\frac{5\pi x_2}{4}) \quad (24)$$

This example was solved by Cheng et al. (2000) using an iterative technique with the DRBEM and CRBFs. However, it should be noted that in this study, the polynomial terms for interpolation were not included, which explains the differences in the quality of the results compared with those in the aforementioned reference. The goal here was to examine the effects of the parameters related to the CRBFs when used with the DIBEM.

As in the previous example, an optimal value of the global percentage error was reached for a value of approximately 80% of complete support, as shown in Figure 15. This result can be attributed to the special behaviour of CRBFs: at values less than the maximum, a better approximation is produced than when using complete support. The error increased less severely above 80% than in the previous example, but a noticeable loss of accuracy occurred between this optimal value and 95% of complete support.

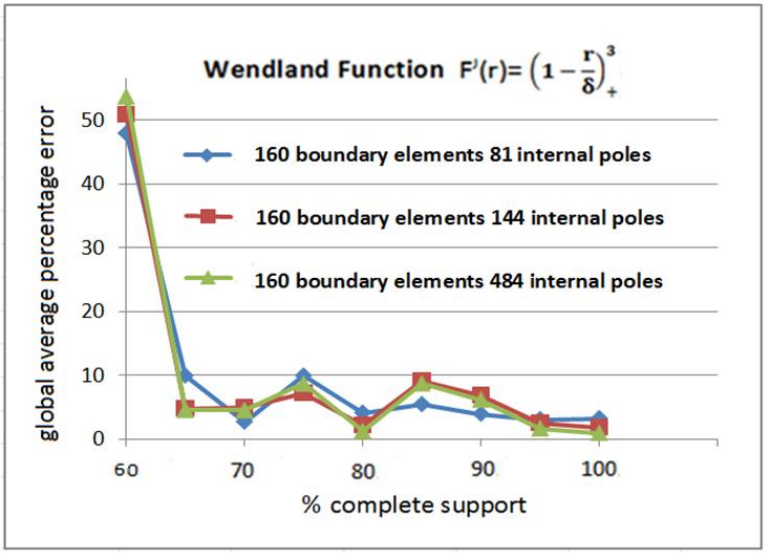

Figure 15: Error in displacements versus the percentage of complete support with three different meshes

9 Conclusions

It can be concluded that the proposed boundary integration scheme has satisfactory performance for simple interpolation problems, since low relative errors were obtained for the volume calculation problems tested. The success of this scheme must be credited to the capability of the primitive CRBFs to provide accuracy despite the boundary transformation required. This type of radial function has performance comparable, or even better, to that of classical radial functions with global support.

In general, the CRBFs with lower order produced greater accuracy because their relative errors were monotonic and the accuracy increased proportionally with the mesh refinement. In this respect, the Wu functions were more prone to instabilities produced by high radial potencies than the Wendland functions.

The amount of internal information is very important for good performance with certain techniques that approximate domain fields. When using the boundary integration scheme, the importance of these internal basis poles is still greater.

However, the value of support radius had a greater effect than the number of basis points on the accuracy of the results of simple interpolation problems. Systematic reduction of support value implies in a continuous increase in errors.

Regarding the use of the boundary integration scheme in conjunction with the BEM, the performance was different from that achieved in the simple interpolation, especially in problems where the distribution of the forcing function was more complicated. In these cases, there seems to be an optimum support value, which in the mathematical formulation is multiplied by the fundamental solution in the kernel of the domain integral. It has been noted in the literature that with domain discretization techniques such as the

FEM, it is possible to improve the accuracy of the results for distorted or discontinuous regions or complex loadings and to effectively avoid the spreading or sharing of effects or properties that are confined to a specific region. Thus, the behaviour exhibited by the proposed technique is not unusual for discrete numerical methods but may be enhanced by the boundary transformation strategy presented here.

The greatest problem is to overcome the significant loss of accuracy produced by the support reduction before reaching the optimal value so that the advantages of using CRBFs can be present in more important applications, particularly those in which the use of radial functions allows the construction of a mass matrix. This is the case in many problems governed by the Helmhotz equation and the wave equation, where a large proportion of the nodal points are typically required for suitable frequency capitation or dynamic simulations. The CRBFs produce arrays with many null elements, which may result in a lower computational cost and may acceptably compensate the loss of accuracy if a concept similar to the finite element lumped mass matrix may be used.

References

Atluri, S. N.; Zhu, T. L. (2000): New Concepts in Meshless Methods. *International Jour nal for Numerical Methods in Engineering*, vol. 47, pp. 537-556.

Brebbia, C. A.; Telles, J. C. F.; Wrobel, L. C. (1984): *Boundary Element Techniques.* Springer-Verlag, Berlin.

Buhmann, M. D. (2003): *Radial Basis Function: Theory and Implementations*. Cambrid ge Press.

Chen C. S.; Brebbia C. A.; Power H. (1999): Dual Reciprocity Method Using Compact ly Supported Radial Basis Functions. *Commun. Numer. Meth. Engng*, vol.15, pp.137-150.

Cheng A. H. D.; Young, D. L.; Tsai, C. C. (2000): Solution of Poisson's Equation by it erative DRBEM using Compactly Supported, Positive Definite Radial Basis Function. *En g. Analysis with Boundary Elements*, vol. 24, pp. 549-557.

Dong, L.; Alotaibi, A.; Mohiuddine, S. A.; Atluri, S. N. (2014): Computational meth ods in engineering: a variety of primal & mixed methods, with global & local interpolatio ns, for well-posed or ill-Posed BCs. *CMES: Computer Modeling in Engineering & Scienc es*, vol. 99, no. 1, pp. 1-85.

Ekhlakov, A. V.; Khay, O. M.; Zhang, C.; Gao, X. W.; Sladek, J.; Sladek, V. (2013): A comparative study of three domain-integral evaluation techniques in the boundary-dom ain integral equation method for transient thermoelastic crack analysis in FGMs. *CMES: Computer Modeling in Engineering & Sciences*, vol. 92, no.6, pp. 595-614.

Fasshauer, G. E. (2007): *Meshfree Approximation Methods with MATLAB. 1ed*. Singapu ra: World Scientific Publishers.

Floater M.; Iske A. (1996): Multistep scattered data interpolation using compactly suppo rted radial basis functions. *J. Comput. and Applied Mathematics*, vol. 73, pp. 65-78.

Franke, R. (1982): Scattered data interpolation: test of some methods. *Mathematics of C omputation*, California, USA, vol. 38, no. 157, pp. 181-200.

Golberg, M. A.; Chen, C. S. (1994): The Theory of Radial Basis Functions applied to th e BEM for Inhomogeneous Partial Differential equations. *BE Communication,* vol.5, pp. 57-61.

Loeffler, C. F.; Cruz, A. L.; Bulcão, A. (2015): A. Direct Use of Radial Basis Interpolat ion Functions for Modelling Source Terms with the Boundary Element Method. *Engineer ing Analysis with Boundary Elements*, vol. 50, pp. 97-108.

Loeffler C. F.; Mansur W. J. (1987): *Analysis of time integration schemes for boundary element applications to transient wave propagation problems.* C.A. Brebbia (Ed.), Boun dary Element Techniques: Applications in Stress Analysis and Heat Transfer, Computatio nal Mechanics Publishing, UK, pp. 105-124.

Partridge, P. W.; Brebbia, C. A.; Wrobel, L.C. (1992): *The Dual Reciprocity Boundar y Element Method.* Computational Mechanics Publications and Elsevier, London.

Sarra, S.A.; Kansa, E. J. (2009): Multiquadric Radial Basis Function Approximation M ethods for the Numerical Solution of Partial Differential Equations. *Advances in Computa tional Mechanics,* Tech Science Press, vol. 2.

Schaback, R. (2007): A practical guide to Radial Basis Functions. http://num.math.uni-g oettingen.de/schaback/teaching/texte/approx/sc.pdf.

Wang, J. G.; Liu, G. R. (2002): A Point Interpolation Meshless Method based on Radial Basis Functions. *International Journal for Numerical Methods in Engineering,* vol.54, p pp. 1623-1648.

Wendland, H. (1995): Piecewise polynomial, positive definite and compactly supported radial functions of minimal degree. *Adv. in Comput. Math*., vol. 4, pp. 389-396.

Wrobel L. C.; Aliabadi, M. H. (2002): *The Boundary Element Method*. Wiley, Chichester.

Wu, Z. (1995): Compactly supported positive definite radial functions. *Adv. in Comput. Math.*, vol. 4, pp. 283-292.